Universiteit Leiden
The Netherlands

Facile generation of heterotelechelic poly(2-oxazoline)s towards accelerated exploration of poly(2-oxazoline)-based nanomedicine

Guyse, J.F.R. van.; Abbasi, S.; Toh, K.; Nagorna, Z.; Li, J.; Dirisala, A.; ... ; Kataoka, K.

Citation
Guyse, J. F. R. van., Abbasi, S., Toh, K., Nagorna, Z., Li, J., Dirisala, A., … Kataoka, K. (2024). Facile generation of heterotelechelic poly(2-oxazoline)s towards accelerated exploration of poly(2-oxazoline)-based nanomedicine. *Angewandte Chemie (International Edition)*, *63*(27). doi:10.1002/anie.202404972

Version:	Publisher's Version
License:	Creative Commons CC BY 4.0 license
Downloaded from:	https://hdl.handle.net/1887/4082204

Note: To cite this publication please use the final published version (if applicable).

How to cite: *Angew. Chem. Int. Ed.* **2024**, *63*, e202404972
doi.org/10.1002/anie.202404972

Polymer Chemistry

Facile Generation of Heterotelechelic Poly(2-Oxazoline)s Towards Accelerated Exploration of Poly(2-Oxazoline)-Based Nanomedicine

Joachim F. R. Van Guyse[+], Saed Abbasi[+], Kazuko Toh, Zlata Nagorna, Junjie Li, Anjaneyulu Dirisala, Sabina Quader, Satoshi Uchida, and Kazunori Kataoka**

Abstract: Controlling the end-groups of biocompatible polymers is crucial for enabling polymer-based therapeutics and nanomedicine. Typically, end-group diversification is a challenging and time-consuming endeavor, especially for polymers prepared via ionic polymerization mechanisms with limited functional group tolerance. In this study, we present a facile end-group diversification approach for poly(2-oxazoline)s (POx), enabling quick and reliable production of heterotelechelic polymers to facilitate POxylation. The approach relies on the careful tuning of reaction parameters to establish differential reactivity of a pentafluorobenzyl initiator fragment and the living oxazolinium chain-end, allowing the selective introduction of N-, S-, O-nucleophiles via the termination of the polymerization, and a consecutive nucleophilic para-fluoro substitution. The value of this approach for the accelerated development of nanomedicine is demonstrated through the synthesis of well-defined lipid-polymer conjugates and POx-polypeptide block-copolymers, which are well-suited for drug and gene delivery. Furthermore, we investigated the application of a lipid-POx conjugate for the formulation and delivery of mRNA-loaded lipid nanoparticles for immunization against the SARS-COV-2 virus, underscoring the value of POx as a biocompatible polymer platform.

Introduction

Accurate control and modulation of polymer termini are key in the application of polymers in biomedicine, which is best exemplified by PEGylation,[1–5] where the polymer termini are exploited to conjugate proteins,[6] nucleic acids,[7] targeting ligands or form nanoassemblies.[8–10] Poly(ethylene glycol) (PEG) enhances water solubility, colloidal stability and provides protection from unwanted recognition by the immune system.[11] The simple conjugation of non-immunogenic, biocompatible (i.e., "stealth") polymers is therefore a widespread and attractive approach to modulate the biodistribution of therapeutics. Another class of polymers well-suited for this purpose are poly(2-oxazoline)s (POx) and their structural relatives, i.e. poly(cyclic imino ether)s, which feature a high degree of structural versatility by merit of the variable ring-size and substituents of the cyclic imino ether monomers.[12–15] In addition to monomer design, a plethora of post-polymerization modification chemistries are available to facilitate further tailoring of the polymer backbone to the needs of specific applications,[16–20] such as tissue engineering and drug delivery.[21–27] Hence, POxylated drug delivery systems enable the fine-tuning of pharmacokinetics and dynamics by modulation of the polymer structure, as well as the attachment of targeting or drug moieties on the backbone, a feature lacking in PEGylated bioconjugates. Although the structural variation along the POx backbone presents ample opportunities in biomedicine, facile end-

[*] Dr. J. F. R. Van Guyse,[+] Dr. S. Abbasi,[+] Dr. K. Toh, Dr. J. Li, Dr. A. Dirisala, Dr. S. Quader, Dr. S. Uchida, Prof. Dr. K. Kataoka
Innovation Center of NanoMedicine
Kawasaki Institute of Industrial Promotion
3-25-14, Tonomachi, Kawasaki-ku, 210-0821 Kawasaki, Japan
and
Present Adresses: S. A.: Center for Nanomedicine at the Wilmer Eye Institute, Johns Hopkins University School of Medicine, 21231 Baltimore, MD, USA
E-mail: j.f.r.van.guyse@lacdr.leidenuniv.nl
kkataoka@g.ecc.u-tokyo.ac.jp

Dr. J. F. R. Van Guyse,[+] Z. Nagorna
Leiden Academic Centre for Drug Research (LACDR)
Leiden University
Einsteinweg 55, 2333 CC Leiden, The Netherlands

Dr. J. Li
Institute for Materials Chemistry and Engineering
Kyushu University
744 Motooka, Nishi-ku, 819-0395 Fukuoka, Japan

Dr. S. Uchida
Department of Medical Chemistry, Graduate School of Medical Science
Kyoto Prefectural University of Medicine
606-0823 Kyoto, Japan

Dr. S. Uchida
Department of Advanced Nanomedical Engineering, Medical Research Institute
Tokyo Medical and Dental University (TMDU)
113-8510 Tokyo, Japan

[+] Both authors contributed equally.

© 2024 The Authors. Angewandte Chemie International Edition published by Wiley-VCH GmbH. This is an open access article under the terms of the Creative Commons Attribution License, which permits use, distribution and reproduction in any medium, provided the original work is properly cited.

© 2024 The Authors. Angewandte Chemie International Edition published by Wiley-VCH GmbH

group diversification remains a key step in the development of advanced drug delivery systems.

In this respect, considerable efforts have been focused on introducing various termini to POx,[28,29] but the process of end-group diversification is typically synthetically exhaustive, and frequently not quantitative, leading to incomplete functionalization (Figure 1).[30,31] Therefore, a strategy that focuses on the post-polymerization diversification of a single end-group is synthetically more attractive, enabling prompt, divergent, yet highly reproducible synthesis. So far, only a handful of functional groups (azides, alkynes, esters, alkenes) can be directly introduced on the α-terminus without protecting groups to facilitate end-group diversification via post-polymerization modification. These functional groups are, however, poorly suited for the introduction of relatively simple molecules with diverse functionalities, *viz.* azide-alkyne cycloadditions are better suited for bioconjugation purposes, non-activated esters are relatively poor electrophiles,[32] whilst the reaction trajectory of radical thiol-ene is concentration dependent (see Supporting Information). In the meanwhile, the difficulty of end-group diversification of the α-terminus is contrasted by the facile end-group diversification of the ω-terminus, whereby the electrophilic 2-oxazolinium can be ring-opened with a wide variety of commercially available O-, N-, or S-based nucleophiles. Inspired by the simplicity and broad scope of the nucleophilic termination reaction, we sought to initiate the cationic ring-opening polymerization (CROP) with a latent electrophilic moiety, susceptible to nucleophilic substitution with a similar substrate scope. In this work, we demonstrate excellent chemoselectivity between the living electrophilic 2-oxazolinium ω-terminus and an electrophilic pentafluorophenyl α-terminus for a variety of nucleophiles via tuning of the reaction parameters. Subsequently, the intact pentafluorophenyl moiety underwent a selective para-fluoro substitution with O-, N-, and S-nucleophiles, thus enabling facile end-group diversification and yielding a wide array of POx functionalized with thioether, amine, or azide ends.

Given the importance of heterotelechelic PEGs in nanomedicine,[33–35] and literature highlighting POx as a viable alternative,[35–38] we explored the synthesis of prototype drug and gene-delivery vehicles, namely block-copolymers, liposomes, and lipid-based nanoparticles (LNPs), by introducing a POx-conjugate synthesized by the pentafluorophenyl chemistry proposed herein. The liposomes prepared using these novel POx-lipids exhibited prolonged circulation following intravenous injection for several hours, confirming the stealth effect of POx when successfully grafted on the surface of nano-assemblies. Importantly, we report on the first application of a lipid-POx conjugate for the formulation and delivery of mRNA-LNPs, which were not inferior to PEG in terms of gene expression in the liver. We also show that POx-lipids can be used as the stabilizer in mRNA vaccines and induce robust cellular and humoral immunity against spike protein of the Coronavirus Disease 2019 (COVID-19). The findings of this study provide an easy and versatile method for the end-group diversification of

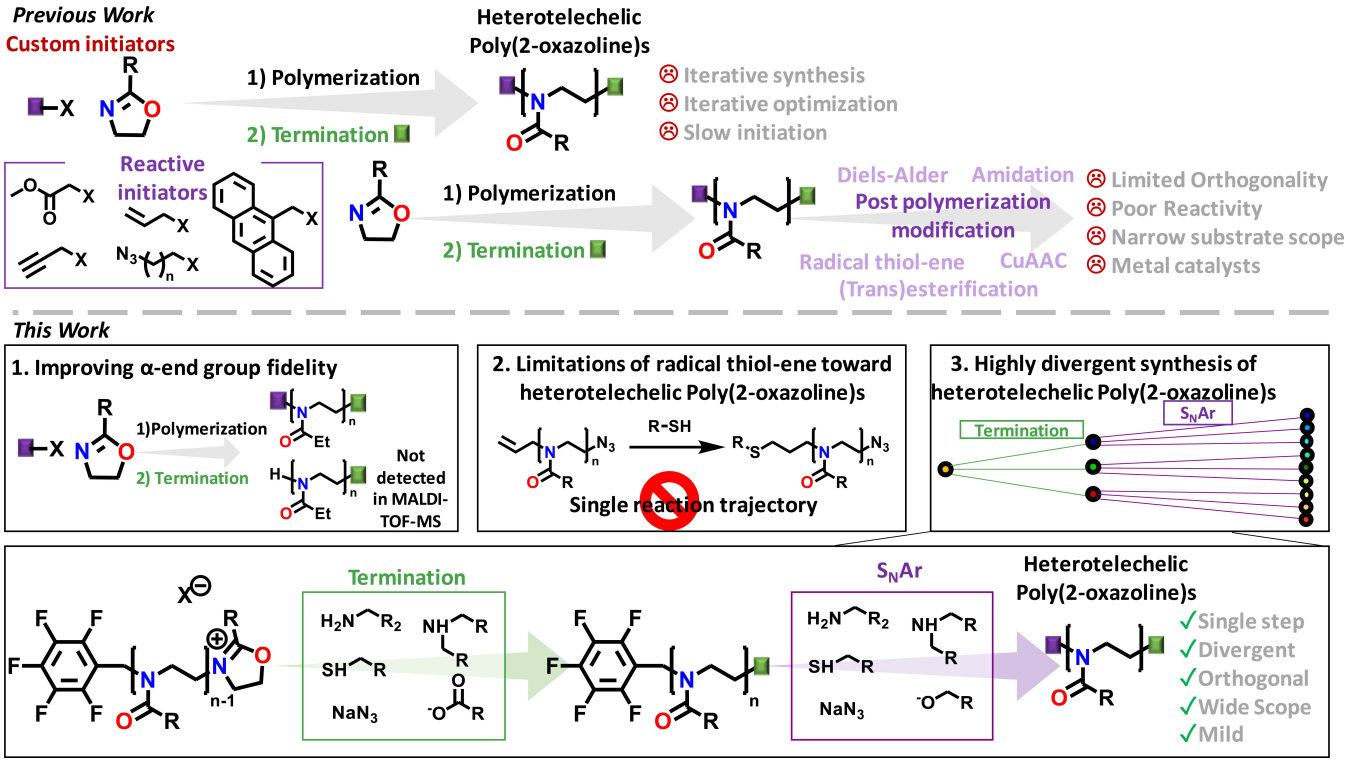

Figure 1. Schematic overview of the synthesis of heterotelechelic poly(2-oxazoline)s whereby previous approaches are iterative or suffer from poor reactivity or substrate scopes. Current work presents a simple and versatile approach for the expeditious generation of heterotelechelic poly(2-oxazoline)s.

© 2024 The Authors. Angewandte Chemie International Edition published by Wiley-VCH GmbH

15213773, 2024, 27, Downloaded from https://onlinelibrary.wiley.com/doi/10.1002/anie.202404972 by Leiden University Libraries, Wiley Online Library on [29/07/2024]. See the Terms and Conditions (https://onlinelibrary.wiley.com/terms-and-conditions) on Wiley Online Library for rules of use; OA articles are governed by the applicable Creative Commons License

poly(cyclic imino ethers), which will have a tremendous advantage on the synthesis of advanced drug delivery systems, benefitting from the stealth effect of the polymer chain and its reactivity to attach targeting moieties on the backbone with more freedom compared to PEG.

Results and Discussion

Reactive Heterotelechelic POx

The large structural diversity of the POx backbone gives a clear incentive for the development of nanomedicine applications, on the condition that heterotelechelics can be obtained with high end-group fidelity, conform to heterotelechelic PEGs. Previous studies, however, have shown the presence of H-initiated species, typically seen in MALDI-TOF-MS spectra,[21,22,39,40] which compromise the end-group fidelity on the α-end. These H-initiated species arise due to chain transfer reactions over the course of the CROP, either via intrinsic chain transfer, i.e. beta-elimination, or extrinsic chain transfer, i.e. impurities. Recent research has indicated that these species can contribute up to 20 mol % of the final product,[30] which severely limits the synthetic utility of the α-end, and POx in general. Indeed, we observed such species in MALDI-TOF-MS spectra, even when the polymerization was performed at low temperatures to limit chain transfer ($Đ < 1.10$),[41–43] with reagents purified according to literature. Gratifyingly, we found that optimized purification of reagents led to the reduction of H-initiated species, as they could no longer be detected by MALDI-TOF-MS, whilst the $Đ$ fell below 1.05 for degrees of polymerization (DP) 90, thus corroborating the purity of the obtained polymers. Furthermore, under these conditions, even a 42 kDa POx could be successfully ionized in reflector mode, representing the highest reported Mw for POx via MALDI-TOF-MS to date (Figure S2A–C).

With these optimized conditions in hand, we explored the development of reactive heterotelechelic POx. Initially, we explored radical thiol-ene chemistry to enable end-group diversification under mild conditions, which in theory allows diversification of the α-end with a variety of commercially available thiols. However, the thiol-ene chemistry was associated with significant formation of side products and low isolated yields (see Supporting Information, section 3), which is presumably caused by the too low concentration of reactants to support radical propagation,[44] seemingly limiting the practical application of thiol-ene chemistry to low molecular weight polymers. To address these shortcomings, we explored the use of pentafluorobenzyl-based initiators, as pentafluorophenyl (PFP)-groups, such as poly(pentafluorostyrene) or poly(pentafluorobenzyl acrylates), have been shown to be reactive to a wide range of substrates, reacting with high efficiency with a variety of N-, O- and S-nucleophiles in a single reaction trajectory, *viz.* a para-fluoro substitution.[45–51] This chemistry, therefore, would be an attractive approach for the α-end-group diversification of POx, as long as the PFP-groups are unreactive towards the N-, O- and S-nucleophiles employed in the termination step of the cationic ring-opening polymerization (CROP). An additional complication is that the termination step of the CROP typically requires the addition of excess of the N-, O- or S- nucleophiles to ensure quantitative reaction,[52–58] and avoid undesired side-reactions, such as overalkylation in the case of amines.[59] Thus far, its exploration in the polymerization of 2-oxazolines has been limited to the synthesis of (multi)blockcopolymers by a condensation reaction of the 2-oxazolinium and pentafluorobenzyl chain ends with bis-or multifunctional thiols,[60] presumably due to a lack of chemoselectivity between the termination reaction and the para-fluoro-substitution under the investigated conditions (vide infra). While the authors claimed that termination with KOH in MeOH proceeds in a selective fashion leaving the PFP moiety intact, our more detailed investigation via ^{19}F NMR indicates otherwise, even when the terminator is applied under substoichiometric conditions (Figure S3A). These results indicate the challenging nature of facilitating chemoselectivity between the 2-oxazolinium species and PFP-groups in the termination reaction and highlight the value of combining multiple characterization techniques to assess chemoselectivity. Hence we investigated the polymerization kinetics and termination of pentafluorobenzyl bromide/tosylate initiated 2-oxazoline polymerizations under different experimental conditions (reaction time, temperature, and solvent), to enable selective termination of the living 2-oxazolinium chain end with different N-, O-, and S-nucleophiles, consequently affording the first heterotelechelic POx bearing the PFP-moiety at the α-end, and azide, amine, ester or thioether groups at the ω-end. In addition, we also describe the derivatization of these heterotelechelics via para-fluoro substitution to obtain novel heterotelechelic combinations.

Polymerization kinetics and Selective termination. Starting with the commercially available pentafluorobenzyl bromide or tosylate, we briefly investigated the polymerization kinetics of 2-ethyl-2-oxazoline (EtOx) in MeCN (Figure S1). Both initiators displayed fast initiation, linear first order kinetics, and a quasi-living polymerization process, despite earlier claimed slow initiation for bromide-based initiators.[53,60] For further reading we refer the reader to section 3 of the Supporting Information. Next, we investigated the selective termination of the living polymer chains by sodium azide, as both the 2-oxazolinium and the PFP moieties have been shown to efficiently react with the azide anion upon mild heating in dipolar aprotic solvents,[47,52] thus presenting an ideal starting point to probe the differential reactivity of both electrophiles. Towards this end, the polymerization of (EtOx) was initiated with pentafluorobenzyl bromide in acetonitrile (MeCN), and the polymerization was allowed to proceed at 70 °C until a monomer conversion of >90 % was reached. Next, 10 molar equivalents of NaN_3 relative to the initiator were added to the polymerization mixture, and the mixture was left to stir at room temperature and periodically sampled to monitor the conversion of the PFP moiety by ^{19}F NMR (Figure S3). Initially, the characteristic ^{19}F signals for the intact PFP moiety are observed. Please note that splitting of the signal occurs due to slow cis/trans-isomerization of the amide bond on NMR

© 2024 The Authors. Angewandte Chemie International Edition published by Wiley-VCH GmbH

15213773, 2024, 27, Downloaded from https://onlinelibrary.wiley.com/doi/10.1002/anie.202404972 by Leiden University Libraries, Wiley Online Library on [29/07/2024]. See the Terms and Conditions (https://onlinelibrary.wiley.com/terms-and-conditions) on Wiley Online Library for rules of use; OA articles are governed by the applicable Creative Commons License

time scale, and as the reaction time increases, peaks corresponding to the tetrafluorophenyl azide appear, indicating that careful control of the reaction time could allow isolation of the desired heterotelechelic product. This was also confirmed by isolating polymers with different DPs after stirring 16 h in the presence of NaN_3, as can be seen from Figure 2 for a poly(2-ethyl-2-oxazoline) (PEtOx) prepared with an [M]/[I] = 50. Figure S4 shows that the obtained polymer possesses a narrow molecular weight distribution with $Đ = 1.04$, which is in line with dispersity values expected for quasi-living ring-opening polymerizations, while Figure 2 demonstrates that the terminal PFP-groups remained intact. This is further supported by the MALDI-TOF-MS measurements in Figures 2 & S4, where a monomodal mass distribution is obtained, whereby the experimental spectrum closely matches the simulated spectra. The presence of the pentafluorobenzyl group was further confirmed via ^{1}H NMR (Figure S5), due to the characteristic benzyl signals appearing at 4.55–4.75 ppm, whereby the relative ratio of the integral of polymer side-chain CH_3 and pentafluorobenzyl protons (135/3 = 45) exactly matches the DP of the most intense signal observed in MALDI-TOF-MS, $m = 4682.12$ Da, which confirms the absence of side reactions, slow initiation (Figure S1 & Supporting Information, section 3), and the high purity of the obtained product. Similarly, terminating the polymerization with acetate salts also enabled the selective introduction of the corresponding ester at the ω-terminus, demonstrating adequate selectivity under conventional polymerization conditions (Figure S6–7). However, termination of the polymerization with amine or aliphatic thiols under these conditions led to a loss of selectivity, leading to a mixture of heterotelechelic products, regardless of the employed reaction temperature or reaction time (Figure S8). For aliphatic thiols in particular, the para-fluoro-substitution took place before quantitative reaction with the 2-oxazolinium species (Figure S9–10).

To address this issue, we hypothesized that selective termination could be facilitated if the involved transition states could be energetically discriminated, namely the 2-oxazoliunium species, and the formed Meisenheimer complex in the nucleophilic aromatic substitution. We rationalized that this could be achieved by switching to an apolar polymerization solvent, as the activation energy for propagation in the CROP, and presumably termination, drops in apolar solvents,[43] while the formation of the Meisenheimer complex is energetically disfavored in apolar solvents due to a lack of stabilizing dipolar interactions. To our delight, performing the polymerization in chlorobenzene with the commercially available PFBz-OTs as initiator allowed the selective termination and isolation of the desired heterotelechelic products (Figure 2). For full experimental and characterization details, we refer the reader to the Supporting Information (Figures S11–14). We should, however, acknowledge that the use of PFBz-OTs as initiator in PhCl exhibits slow initiation of the CROP (Figure S1, Supporting Information section 3), an issue that can be addressed by increasing the reaction temperature,[63] the addition of triflate salts, or the use of the corresponding oxazolinium salts as initiators.

Para-fluoro Substitution. With these reactive heterotelechelic POx in hand, we subsequently explored their derivatization for facile end-group diversification. Initially, the azide fluoro-substitution was performed in order to further

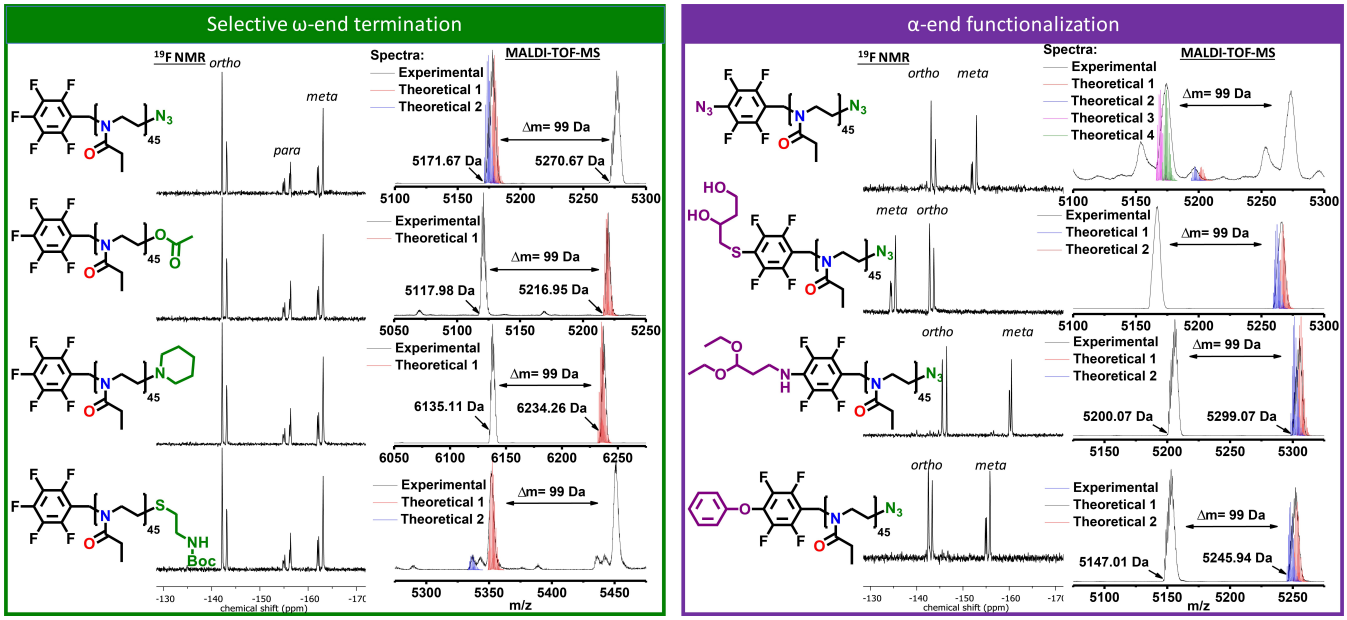

Figure 2. Overview of representative examples of selective ω-end termination and α-end functionalization performed in this work, corroborated by the corresponding ^{19}F NMR and MALDI-TOF-MS spectra of the given structures. Experimental monoisotopic masses are only given for spectra with sufficient resolution, theoretical spectra account for known fragmentation patterns of azides and boc-groups.[61,62] For comprehensive analysis and additional examples the reader is referred to the Supporting Information.

© 2024 The Authors. Angewandte Chemie International Edition published by Wiley-VCH GmbH

15213773, 2024, 27, Downloaded from https://onlinelibrary.wiley.com/doi/10.1002/anie.202404972 by Leiden University Libraries, Wiley Online Library on [29/07/2024]. See the Terms and Conditions (https://onlinelibrary.wiley.com/terms-and-conditions) on Wiley Online Library for rules of use; OA articles are governed by the applicable Creative Commons License

prove the purity of the polymers synthesized in the previous section. Here, we adjusted the conditions reported by Noy et al.[47] to obtain a PEtOx with two azide end-groups, *viz.* an alkyl azide and a tetrafluorophenylazide terminus. The transformation proceeded in a controlled fashion, as the DMF-GPC (Figure S15) showed a comparable molecular weight distribution to that of the starting material, with no evidence of chain coupling reactions. Furthermore, the ^{19}F NMR clearly showed only two ^{19}F signals, indicating that indeed the fluor in para-position was solely substituted, and that para-substituted tetrafluorphenyl azides were formed, which was also evident from the chemical shift of the meta-fluorines (Figure 2). Finally, MALDI-TOF-MS further supported the formation of the product, as the peaks corresponding to the expected fragmentation products were present in the experimental spectrum (Figure 2). It should be noted, however, that additional product peaks were present, which could not be identified. These peaks presumably arise from the photochemical transformation of the para-substituted tetrafluorophenyl azides,[64] which is induced by the laser irradiation under the experimental conditions, thus yielding highly reactive nitrenium ions which can react with the matrix. Nevertheless, these results further confirm that selective azide termination is possible, as well as demonstrate that highly reactive para-substituted tetrafluorphenyl azides can be formed, which could be potentially employed in photochemical transformations or azide-alkyne cycloadditions.[65–67] Next, we focused on the base-catalyzed para-fluoro thiol substitution as a large variety of commercially available thiols could potentially be coupled under relatively mild conditions. A screening experiment indicated that triethylamine could successfully catalyze the coupling of aliphatic thiols, such as 1-thioglycerol, if significant excess of base and thiol (6 and 5 equivalents relative to PFP) were applied in DMF, in combination with mild heating and prolonged reaction times (16 h, 60 °C). Nonetheless, the reactions were successful as the characteristic product peaks could be seen in MALDI-TOF-MS and ^{1}H and ^{19}F NMR (Figure S16). Although successful, KOtBu as a base was found to be more potent (Table S2), as the reaction was completed within 1 hour at room temperature by employing 5 equivalents of thiol and 4 equivalents of base. Unfortunately, attempts to reduce the molar excess of base and thiol were unsuccessful, as the reaction did not reach full conversion even after 4 days. Hence, DBU was explored as a catalyst, enabling full conversion of the PFP moiety within 1 hour at room temperature with as little as 1.35 equivalents of DBU and 1.5 equivalents of thiol (Figure 2). Nevertheless, the screening of different thiols revealed that 2 equivalents of thiol and 1.8 equivalents of DBU presented optimal conditions for a broad variety of thiols, including mercaptoethanol, cysteamine, mercaptopropionate and 1-thioglucose tetra acetate (Figures S17–S24). Of note is that thiolates can also reduce alkyl azides,[68–70] however under the employed reaction conditions no reduction towards amines was noted via analytical ion exchange chromatography (Figure S25), suggesting that the reduction is kinetically not relevant under these conditions.

Having demonstrated the successful modification with thiols and azides, we subsequently explored the para-fluoro substitution with various amines. Initially, we adopted the conditions of Noy et al.,[38] however, it became apparent that these conditions went paired with significant formation of side-products. A screening experiment suggested that the side-products were formed as a result of the thermal and base-induced decomposition of DMF, whereby the in situ generated *N,N*-dimethylamine effectively competed with the desired amine (see Figure S27). Hence, *N*-methylpyrrolidone (NMP) was selected as a more suitable solvent, thus enabling the efficient introduction of a large variety of amines, including piperidine, ethanolamine, ethylenediamine, 3-aminopropionaldehyde diethylacetal, and hydrazine. In Figure 2, the characterization for the 3-aminopropionaldehyde diethylacetal substituted polymer is shown as a representative example, while the other examples are shown in Figures S28–34.

Finally, alkoxides were explored as a last set of substrates in the para-fluoro substitution. Here, phenol was chosen as a model compound, whereby the corresponding alkoxide was generated by in situ deprotonation with triazabicyclodecene (TBD) as a base. The reaction was shown to proceed with mild stoichiometric excess at room temperature in NMP for 24 hours. As is evident from the data in Figures 2 & S35–36, the transformation proceeded smoothly without noticeable side-reactions, as the DMF-GPC still showed the characteristic narrow molecular weight distribution, while the ^{19}F NMR showed the expected signals corresponding to the ortho- and meta-fluorines. Finally, the MALDI-TOF-MS spectra provide conclusive proof that the desired compound was obtained, further demonstrating the absence of side-reactions.

Exploration of Pentafluorophenyl-Functional POx in Nanomedicine Applications

Having demonstrated both the selectivity and versatility of PFP chemistry and its use for other POx and different molecular weights (Figures S46–S50), we subsequently applied it to the synthesis of constructs for nanomedicine. First, we synthesized α-amine and ω-azide heterotelechelic POx through selective azide termination of the CROP and subsequent para-fluoro substitution with excess ethylenediamine. These polymers were subsequently utilized as macroinitiators for the ring-opening polymerization of N-carboxyanhydrides, thus yielding defined N_3-POx-polypeptide block-copolymers ($Đ < 1.10$) as shown in Figure S37. These polymers are well-positioned for nanomedicine research,[71] which is currently ongoing, given the success of N_3-PEG-polypeptide block-copolymers in pre-clinical and clinical trials.[35,72] In addition to well-defined block-copolymers, we explored the synthesis of POx-lipid conjugates, as polymer-lipid conjugates have garnered spotlight attention in recent years as a crucial component in lipid-based gene-delivery systems. Utilizing the 1-thioglycerol modified PFP-POx-N_3 as a precursor, various lipids could be efficiently introduced through a simple Steglich esterification with the correspond-

© 2024 The Authors. Angewandte Chemie International Edition published by Wiley-VCH GmbH

15213773, 2024, 27, Downloaded from https://onlinelibrary.wiley.com/doi/10.1002/anie.202404972 by Leiden University Libraries, Wiley Online Library on [29/07/2024]. See the Terms and Conditions (https://onlinelibrary.wiley.com/terms-and-conditions) on Wiley Online Library for rules of use; OA articles are governed by the applicable Creative Commons License

ing fatty acids. Two lipid conjugates were synthesized utilizing oleic acid (DO) as the lipid tail with different polymer chains, yielding DO-PEtOx-N_3 and DO-PMeOx-N_3 (Figure 3A–B and Figure S38–41). These lipids were formulated in liposomes composed of 1,2-dioleoyl-sn-glycero-3-phosphocholine (DOPC)/Cholesterol/dioleate (DO)-POx in a 62.5/32.5/5 molar by a thin-film hydration method and subsequent extrusion for size control.

Through this method, well-defined liposomes were obtained with a hydrodynamic radius of 127 nm and 143 nm for the DO-PEtOx and DO-PMeOx formulations, respectively (Figure 3D–E). Next, fluorescently labeled liposomes were prepared by incorporating 0.3 mol % of the lipophilic dioctadecyl-3,3,3 3 tetramethylindodicarbocyanine dye (DiD) in the formulations, and their circulation was

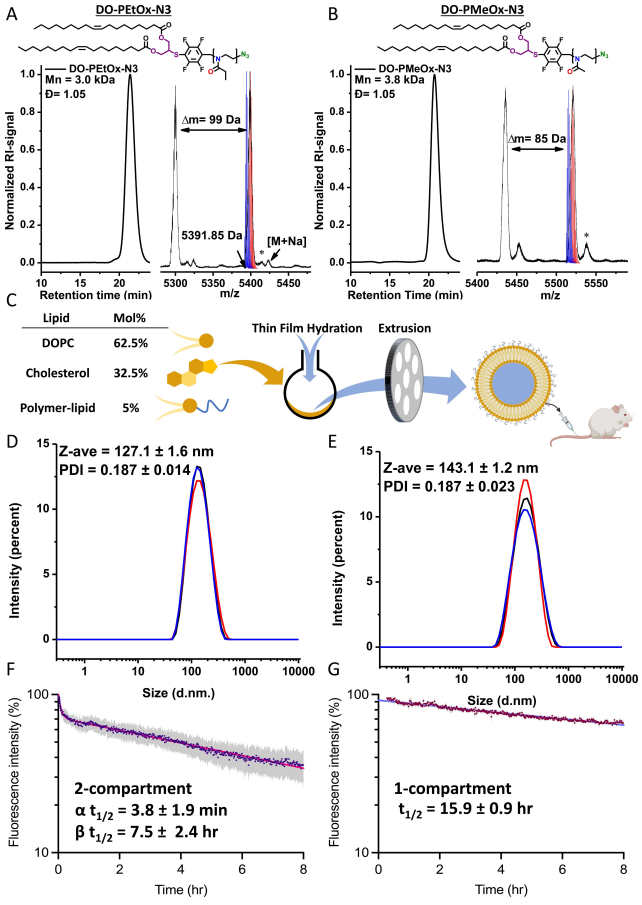

Figure 3. Generation of polymer-lipids and their use in stealth liposomes. A + B) SEC elugram and zoom of experimental MALDI-TOF-MS spectrum (black) of dioleyl-functional PEtOx and PMeOx, respectively. Red and blue signals denote theoretical spectra, while * denotes oxidized product. C) Schematic representation of liposome preparation with the respective molar ratios of each component. D + E) Intensity-based size distribution obtained from DLS for PEtOx- and PMeOx-functionalized liposomes, respectively ($n = 3$ for each plot). F + G) Fluorescence intensity in murine ear-lobe vein relative to tissue as a function of time after administration of DiD-labeled PEtOx- and PMeOx-functional liposomes, respectively ($n = 3$ for each plot). Data represented as the mean ± SEM ($n = 3$). Error bands are highlighted in gray.

observed by intravital confocal laser scanning microscopy. Both liposome formulations containing either PEtOx or PMeOx showed prolonged circulation following intravenous injection in mice. Interestingly, PMeOx showed a first order one-compartment elimination kinetics, compared to PEtOx which showed a rapid drop followed by slow elimination that fits well into a 2-compartment elimination model. This could be attributed to the higher hydrophilicity of PMeOx, providing the liposome surface a better stealth effect against elimination, whereas the PEtOx liposomes can be considered as pseudo-stealth.[73] Importantly, however, the observed blood circulation profiles correspond well to the obtained half-lives of earlier reported POx-liposomes,[74] which do not utilize this tetrafluorophenyl (TFP) linker technology, thus indicating that this linker has a negligible influence on the pharmacokinetics of the liposome in mice.

Lipid-based nanoparticle (LNP) mediated mRNA delivery. In contrast to the prevalently used PEG-lipids, our system has a hydrophobic TFP linker between polymer and lipid components. The two liposomes used in Figure 3 displayed long blood circulation, indicating that the linker has negligible effects on the liposome behavior in the blood. However, the hydrophobic linker could influence the functionality of lipid-based nanoparticles (LNPs) when the desorption of polymer-lipids is needed in the blood. In LNP-mediated small interfering RNA (siRNA) delivery, the hepatic gene knockdown was superior for dimyristyl (C14)-functional PEG relative to distearyl (C18)-functional PEG, which correlates with their desorption rate in plasma, 45 %/h and 0.2 %/h, respectively.[75] Similar effects have been observed in the LNP-mediated delivery of mRNA,[76] indicating the importance of the lipid-polymer design for efficient RNA delivery. In such settings, the hydrophobic TFP linker may impair LNP function by inhibiting the desorption of PEtOx-lipid. Therefore, we tested the functions of PEtOx-lipid in the systemic administration of mRNA LNPs, which could require desorption of PEtOx-lipid in the blood to obtain protein expression in the liver and other organs. mRNA LNPs were formulated from POx-lipids featuring different fatty acid tails, D-Lin-MC3-DMA (MC3) as ionizable cationic lipid, DSPC, and cholesterol as helper lipids. The commercial 1,2-dimyristoyl-rac-glycero-3-methoxypolyethylene glycol (DMG-PEG) (C14) lipid, a widely used component of siRNA and mRNA LNPs, was set as a benchmark. In short, mRNA was formulated with either DMG-PEG, dimyristyl (DM)-PEtOx-N_3 (Figure S42–43) or DO-PEtOx-N_3, whereby the polymers displayed comparable chain lengths of 45 repeating units. Utilizing microfluidics, LNPs were obtained with a narrow size-distribution around 70–80 nm as measured by DLS, with comparable mRNA encapsulation efficiencies (Table S3), all of which were stable for at least 7 days (Figure S44). Next, the formulated LNPs were intravenously injected into mice, and the protein expression was assessed using IVIS in live mice and the isolated major organs (Figure 4). Figure 4B–E shows that DM-PEtOx was able to elicit comparable mRNA introduction efficiency in the liver to the commercially available DMG-PEG, despite the presence of the hydrophobic TFP linker in the former. This result suggests that

© 2024 The Authors. Angewandte Chemie International Edition published by Wiley-VCH GmbH

15213773, 2024, 27, Downloaded from https://onlinelibrary.wiley.com/doi/10.1002/anie.202404972 by Leiden University Libraries, Wiley Online Library on [29/07/2024]. See the Terms and Conditions (https://onlinelibrary.wiley.com/terms-and-conditions) on Wiley Online Library for rules of use; OA articles are governed by the applicable Creative Commons License

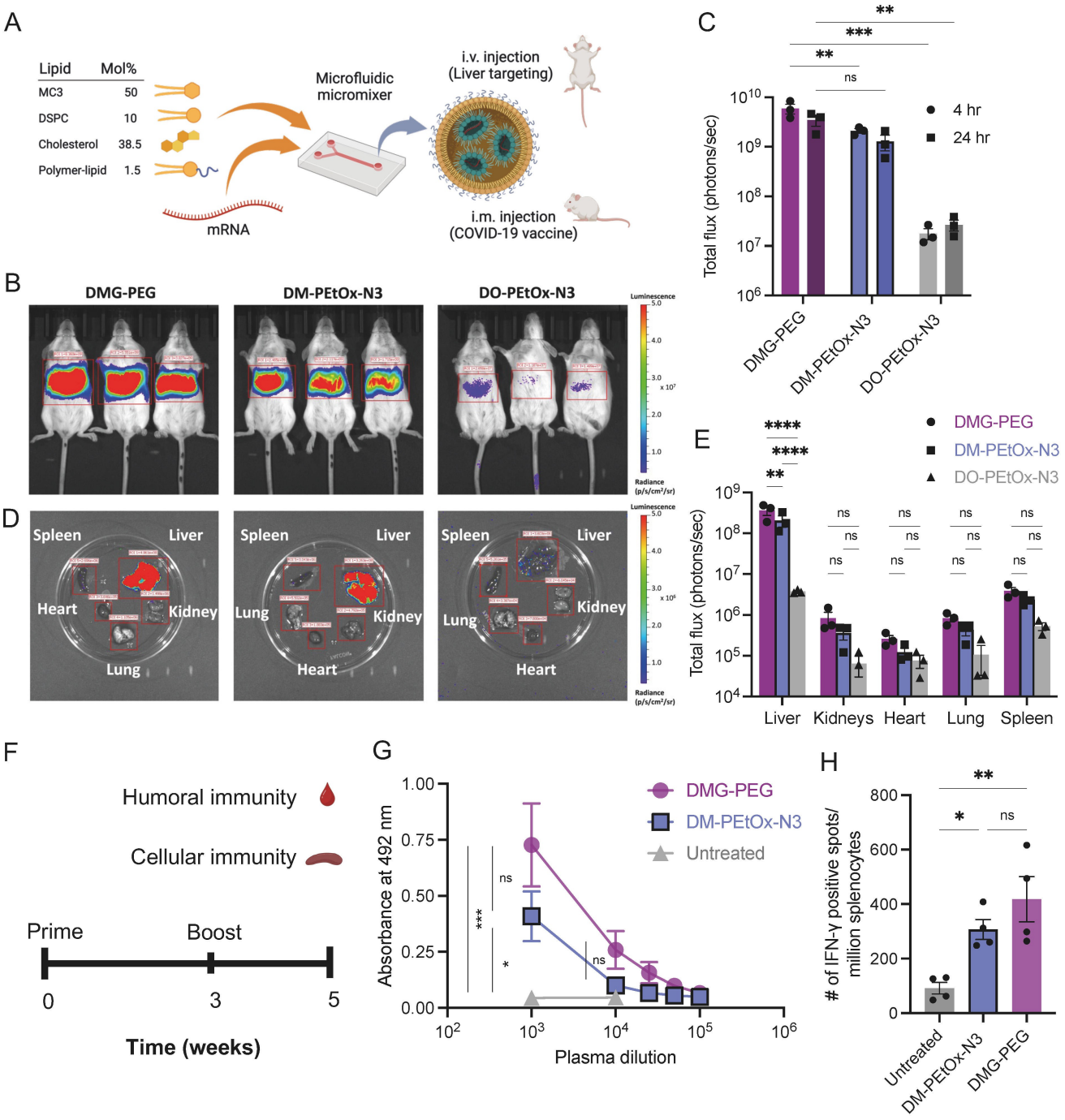

Figure 4. Generation of POXylated LNPs for mRNA delivery in-vivo. A) Preparation of mRNA-loaded LNPs using microfluidic mixing. B) Firefly luciferase expression in Balb/C mice injected intravenously with LNPs 4 h post-injection. C) Quantification of the firefly luciferase expression in Balb/C mice injected intravenously with LNPs 4 h and 24 post-injection ($n=3$). Data represented as the mean (+/-) SEM. Two-way ANOVA followed by Tukey's test. *$p<0.05$, **$p<0.01$. ***$p<0.001$, ****$p<0.0001$, ns: non-significant. D) Biodistribution of firefly luciferase expression in major organs isolated from Balb/C mice injected intravenously with LNPs 24 h post-injection. E) Quantification of the firefly luciferase expression in the organs 24 h post-injection, as assessed by ex vivo measurements ($n=3$). F) Immunization of mice with DMG-PEG and DM-PetOx-N3 LNPs featuring the SARS-COV-2 spike protein-encoding mRNA following a prime-boost administration schedule. G) Spike protein-specific IgG production. H) Induction of cellular immunity in spleens of vaccinated mice ($n=4$). Data represented as the mean (+/-) SEM. One-way ANOVA followed by Tukey's test. *$p<0.05$, **$p<0.01$. ***$p<0.001$, ****$p<0.0001$, ns: non-significant.

neither POx chains nor the TFP-linker largely impairs the mRNA delivery process to the major organs and that the TFP-linker can be successfully applied in settings where lipid-desorption is required. While DM-PEtOx was able to provide considerable gene expression, the in vivo protein expression levels for DO-PEtOx were limited. Presumably,

© 2024 The Authors. Angewandte Chemie International Edition published by Wiley-VCH GmbH

15213773, 2024, 27, Downloaded from https://onlinelibrary.wiley.com/doi/10.1002/anie.202404972 by Leiden University Libraries, Wiley Online Library on [29/07/2024]. See the Terms and Conditions (https://onlinelibrary.wiley.com/terms-and-conditions) on Wiley Online Library for rules of use; OA articles are governed by the applicable Creative Commons License

these limited expression levels originate from the higher membrane association of DO-PEtOx, relative to DM-PEtOx and DMG-PEG. Besides gene expression, the toxicity of all formulations was investigated by measuring different plasma biochemical markers of the liver and kidney relative to mice injected with PBS (Figure S45). These results indicate the potential of the investigated polymer lipids as an alternative to PEG-lipids, although further optimization, including PEtOx lengths, is needed to identify optimal compositions for specific applications.[77]

Finally, since the newly developed POx-lipids displayed excellent potential for the delivery of mRNA, we assessed the potential of the DM-PEtOx formulation in the administration of mRNA encoding the COVID-19 spike protein, whereby the cellular immunity and antigen-specific antibody production was monitored. Here, mice were intramuscularly (i.m) injected with 5μg of mRNA in a prime-boost series separated three weeks apart. Two weeks after the last dose, blood plasma and spleens were collected for the quantification of humoral and cellular immunity, respectively. Figure 4G–H shows that the DM-PEtOx formulation was able to induce both cellular immunity and antibody production relative to unvaccinated mice, demonstrating the potential of POx-lipids in LNP-vaccination technology. POx can be a potential substitute for those with contraindications to current COVID-19 vaccines due to a history of severe allergy to PEG-lipids, although allergic properties of POx should be thoroughly examined in the future. Additionally, the POx backbone can serve as a versatile platform for attaching targeting moieties to deliver the LNPs to specific cells with more tunability compared to PEG which only allows functionalizing at its terminus.

Conclusion

In summary, we present a simple, single post-polymerization modification step to facilitate the diversification of POx end-groups, potentiating rapid development of heterotelechelic libraries of this structurally diverse polymer class of which we presented a 25-membered example. The presented methodology is in principle orthogonal with several functional groups that have been incorporated along the polymer chain (e.g. esters, alkynes, alkenes, azides),[32,78–80] which we demonstrated for ester functional POx. As demonstrated in this manuscript, the development of such libraries facilitates the exploration of POx into nanomedicine applications, allowing the synthesis of well-defined block-copolymers, polymer-lipid conjugates, as well as polymers with a targeting ligand, such as glucose.[81] We briefly demonstrated the potential of this chemistry in in vivo settings, namely the formulation of liposomes and nucleic acid-loaded lipid nanoparticles. The tetrafluorophenyl linker between polymer and lipid in these formulations was found to have no significant impact on the performance of these formulations in vivo, as the obtained liposomes displayed blood circulation profiles in mice similar to literature reports of analogous structures.[74,82] Furthermore, for LNP-mediated nucleic acid delivery, the presence of this hydrophobic linker did not impair gene expression, as expression levels were similar to those obtained for PEG-lipids, indicating that the in vivo polymer-lipid desorption from the LNPs was not impacted by the hydrophobicity of this linker. Importantly, these novel POx-based formulations did not show any significant toxicological markers relative to PBS, indicating the absence of acute toxicity. Finally, these lipid-POx conjugates were applied in the formulation of SARS-CoV-2 spike mRNA for vaccine development, whereby the new formulations were found to induce cellular immunity and antibody production relative to unvaccinated mice, demonstrating the potential of POx-lipids in LNP-vaccination technology. Notably, the successful formulation of stealth liposomes and mRNA-LNPs that could be used for liver targeting and COVID-19 vaccines with azide-functionalized surfaces is encouraging to further investigate ligand installation in the future.

Supporting Information

The authors have cited additional references within the Supporting Information.[83–95]

Acknowledgements

The authors wish to thank Miki Matsui-Masai, Shigeto Fukushima, and Theofilius A. Tockary for their technical assistance over the course of this research. J. F. R. V. G. and K. K. are grateful for the financial support provided by the Japan Society for the Promotion of Science (Grant P20369) and the Grant-in-Aid for JSPS Fellows (Grant 20F20369) for this research.

Conflict of Interest

J. F. R. V. G., S. A., S. U., and K. K. are listed as inventors on a patent that covers heterotelechelic pentafluorophenyl-functional poly(2-oxazoline)s, their derivatives, and their use in lipid-formulations.

Data Availability Statement

The data that support the findings of this study are available from the corresponding author upon reasonable request.

Keywords: polymer analogous reaction · gene delivery · liposomes · lipid nanoparticles · COVID-19 vaccine

[1] F. M. Veronese, A. Mero, *BioDrugs* **2008**, *22*, 315–329.
[2] E. Blanco, H. Shen, M. Ferrari, *Nat. Biotechnol.* **2015**, *33*, 941–951.
[3] J. S. Suk, Q. Xu, N. Kim, J. Hanes, L. M. Ensign, *Adv. Drug Delivery Rev.* **2016**, *99*, 28–51.

© 2024 The Authors. Angewandte Chemie International Edition published by Wiley-VCH GmbH

15213773, 2024, 27, Downloaded from https://onlinelibrary.wiley.com/doi/10.1002/anie.202404972 by Leiden University Libraries, Wiley Online Library on [29/07/2024]. See the Terms and Conditions (https://onlinelibrary.wiley.com/terms-and-conditions) on Wiley Online Library for rules of use; OA articles are governed by the applicable Creative Commons License

[4] H. Otsuka, Y. Nagasaki, K. Kataoka, *Adv. Drug Delivery Rev.* **2003**, *55*, 403–419.
[5] V. P. Torchilin, *Nat. Rev. Drug Discovery* **2005**, *4*, 145–160.
[6] Y. Wang, C. Wu, *Biomacromolecules* **2018**, *19*, 1804–1825.
[7] N. Yoshinaga, M. Naito, Y. Tachihara, E. Boonstra, K. Osada, H. Cabral, S. Uchida, *Pharmaceutica* **2021**, *13*, DOI 10.3390/pharmaceutics13060800.
[8] B. Wang, C. V. Galliford, P. S. Low, *Nanomedicine* **2014**, *9*, 313–330.
[9] J. Li, K. Kataoka, *J. Am. Chem. Soc.* **2021**, *143*, 538–559.
[10] P. Mi, H. Cabral, K. Kataoka, *Adv. Mater.* **2020**, *32*, 2070101.
[11] A. Jain, S. K. Jain, *Crit. Rev. Ther. Drug Carrier Syst.* **2008**, *25*, 403–447.
[12] B. Verbraeken, J. Hullaert, J. Van Guyse, K. Van Hecke, J. Winne, R. Hoogenboom, *J. Am. Chem. Soc.* **2018**, *140*, 17404–17408.
[13] J. F. R. Van Guyse, R. Hoogenboom, in *Macromol. Eng.*, John Wiley & Sons, Ltd, **2022**, pp. 1–48.
[14] Z. Varanaraja, J. Kim, C. R. Becer, *Eur. Polym. J.* **2021**, *147*, 110299.
[15] A. Zahoranová, R. Luxenhofer, *Adv. Healthcare Mater.* **2021**, *10*, DOI 10.1002/adhm.202001382.
[16] M. W. M. M. Fijten, C. Haensch, B. M. Van Lankvelt, R. Hoogenboom, U. S. Schubert, *Macromol. Chem. Phys.* **2008**, *209*, 1887–1895.
[17] J. F. R. Van Guyse, M. A. Mees, M. Vergaelen, M. Baert, B. Verbraeken, P. J. Martens, R. Hoogenboom, *Polym. Chem.* **2019**, *10*, 954–962.
[18] R. W. Moreadith, T. X. Viegas, M. D. Bentley, J. M. Harris, Z. Fang, K. Yoon, B. Dizman, R. Weimer, B. P. Rae, X. Li, C. Rader, D. Standaert, W. Olanow, *Eur. Polym. J.* **2017**, *88*, 524–552.
[19] T. R. Dargaville, R. Forster, B. L. Farrugia, K. Kempe, L. Voorhaar, U. S. Schubert, R. Hoogenboom, *Macromol. Rapid Commun.* **2012**, *33*, 1695–1700.
[20] A. Sehlinger, B. Verbraeken, M. A. R. Meier, R. Hoogenboom, *Polym. Chem.* **2015**, *6*, 3828–3836.
[21] S. Osawa, K. Osada, S. Hiki, A. Dirisala, T. Ishii, K. Kataoka, *Biomacromolecules* **2016**, *17*, 354–361.
[22] B. S. Kim, S. Osawa, M. Naito, S. Ogura, R. Kamegawa, H. Ishida, H. J. Kim, S. Uchida, K. Miyata, *Adv. Ther.* **2019**, *3*, 1900123.
[23] B. S. Kim, H. J. Kim, S. Osawa, K. Hayashi, K. Toh, M. Naito, H. S. Min, Y. Yi, I. C. Kwon, K. Kataoka, K. Miyata, *ACS Biomater. Sci. Eng.* **2019**, *5*, 5770–5780.
[24] T. Lorson, M. M. Lübtow, E. Wegener, M. S. Haider, S. Borova, D. Nahm, R. Jordan, M. Sokolski-Papkov, A. V. Kabanov, R. Luxenhofer, *Biomaterials* **2018**, *178*, 204–280.
[25] T. R. Dargaville, J. R. Park, R. Hoogenboom, *Macromol. Biosci.* **2018**, *18*, 1–15.
[26] V. R. de la Rosa, *J. Mater. Sci. Mater. Med.* **2014**, *25*, 1211–1225.
[27] O. Sedlacek, V. R. de la Rosa, R. Hoogenboom, *Eur. Polym. J.* **2019**, *120*, 109246.
[28] G. Delaittre, *Eur. Polym. J.* **2019**, *121*, 109281.
[29] B. Guillerm, S. Monge, V. Lapinte, J. J. Robin, *Macromol. Rapid Commun.* **2012**, *33*, 1600–1612.
[30] M. Brunzel, M. Dirauf, M. Sahn, J. A. Czaplewska, N. Fritz, C. Weber, I. Nischang, U. S. Schubert, *J. Chromatogr. A* **2021**, *1653*, DOI 10.1016/J.CHROMA.2021.462364.
[31] Z. A. I. Mazrad, M. Lai, T. P. Davis, J. A. Nicolazzo, K. J. Thurecht, M. N. Leiske, K. Kempe, *Polym. Chem.* **2022**, *13*, 4436–4445.
[32] J. F. R. Van Guyse, Y. Bernhard, A. Podevyn, R. Hoogenboom, *Angew. Chem. Int. Ed.* **2023**, *62*, e202303841.
[33] S. J. Walsh, J. D. Bargh, F. M. Dannheim, A. R. Hanby, H. Seki, A. J. Counsell, X. Ou, E. Fowler, N. Ashman, Y. Takada, A. Isidro-Llobet, J. S. Parker, J. S. Carroll, D. R. Spring, *Chem. Soc. Rev.* **2021**, *50*, 1305–1353.
[34] I. Ekladious, Y. L. Colson, M. W. Grinstaff, *Nat. Rev. Drug Discovery* **2019**, *18*, 273–294.
[35] H. Cabral, K. Miyata, K. Osada, K. Kataoka, *Chem. Rev.* **2018**, *118*, 6844–6892.
[36] M. Barz, R. Luxenhofer, R. Zentel, M. J. Vicent, *Polym. Chem.* **2011**, *2*, 1900–1918.
[37] K. Knop, R. Hoogenboom, D. Fischer, U. S. Schubert, *Angew. Chem. Int. Ed.* **2010**, *49*, 6288–6308.
[38] M. Cárdenas, R. A. Campbell, M. Yanez Arteta, M. J. Lawrence, F. Sebastiani, *Curr. Opin. Colloid Interface Sci.* **2023**, *66*, 101705.
[39] S. Czich, T. Wloka, H. Rothe, J. Rost, F. Penzold, M. Kleinsteuber, M. Gottschaldt, U. S. Schubert, K. Liefeith, *Molecules* **2020**, *25*, DOI 10.3390/molecules25215066.
[40] N. E. Göppert, A. Vollrath, L. M. Stafast, S. Stumpf, B. Schulze, S. Hoeppener, C. Weber, U. S. Schubert, *RSC Appl. Polym.* **2024**, DOI 10.1039/d3lp00085k.
[41] J. S. Park, K. Kataoka, *Macromolecules* **2007**, *40*, 3599–3609.
[42] B. D. Monnery, S. Shaunak, M. Thanou, J. H. G. Steinke, *Macromolecules* **2015**, *48*, 3197–3206.
[43] B. D. Monnery, V. V. Jerca, O. Sedlacek, B. Verbraeken, R. Cavill, R. Hoogenboom, *Angew. Chem. Int. Ed.* **2018**, DOI 10.1002/anie.201807796.
[44] M. D. Nolan, M. Schüttel, E. M. Scanlan, A. L. Nielsen, *Pept. Sci.* **2023**, e24310.
[45] G. Delaittre, L. Barner, *Polym. Chem.* **2018**, *9*, 2679–2684.
[46] J. M. Noy, M. Koldevitz, P. J. Roth, *Polym. Chem.* **2015**, *6*, 436–447.
[47] J. M. Noy, Y. Li, W. Smolan, P. J. Roth, *Macromolecules* **2019**, *52*, 3083–3091.
[48] J. M. Noy, A. K. Friedrich, K. Batten, M. N. Bhebhe, N. Busatto, R. R. Batchelor, A. Kristanti, Y. Pei, P. J. Roth, *Macromolecules* **2017**, *50*, 7028–7040.
[49] D. Varadharajan, G. Delaittre, *Polym. Chem.* **2016**, *7*, 7488–7499.
[50] C. R. Becer, K. Babiuch, D. Pilz, S. Hornig, T. Heinze, M. Gottschaldt, U. S. Schubert, *Macromolecules* **2009**, *42*, 2387–2394.
[51] C. Ott, R. Hoogenboom, U. S. Schubert, *Chem. Commun.* **2008**, 3516–3518.
[52] S. Osawa, T. Ishii, H. Takemoto, K. Osada, K. Kataoka, *Eur. Polym. J.* **2017**, *88*, 553–561.
[53] A. Podevyn, K. Arys, V. R. de la Rosa, M. Glassner, R. Hoogenboom, *Eur. Polym. J.* **2019**, *120*, 109273.
[54] G. Morgese, L. Trachsel, M. Romio, M. Divandari, S. N. Ramakrishna, E. M. Benetti, G. Morgese, L. Trachsel, M. Romio, E. S. Dehghani, J. G. Rosenboom, C. Paradisi, M. Zenobi-Wong, S. N. Ramakrishna, E. M. Benetti, *Angew. Chem. Int. Ed.* **2016**, *55*, 15583–15588.
[55] O. Sedlacek, K. Lava, B. Verbraeken, S. Kasmi, B. G. De Geest, R. Hoogenboom, *J. Am. Chem. Soc.* **2019**, jacs.9b02607.
[56] C. Giardi, V. Lapinte, F. Nielloud, J. M. Devoisselle, J. J. Robin, *J. Polym. Sci. Part A* **2010**, *48*, 4027–4035.
[57] T. X. Viegas, M. D. Bentley, J. M. Harris, Z. Fang, K. Yoon, B. Dizman, R. Weimer, A. Mero, G. Pasut, F. M. Veronese, *Bioconjugate Chem.* **2011**, *22*, 976–986.
[58] C. Weber, M. Wagner, D. Baykal, S. Hoeppener, R. M. Paulus, G. Festag, E. Altuntas, F. H. Schacher, U. S. Schubert, *Macromolecules* **2013**, *46*, 5107–5116.
[59] R. Luxenhofer, G. Sahay, A. Schulz, D. Alakhova, T. K. Bronich, R. Jordan, A. V. Kabanov, *J. Controlled Release* **2011**, *153*, 73–82.
[60] T. Zhao, B. Drain, G. Yilmaz, C. R. Becer, *Polym. Chem.* **2021**, *12*, 6392–6403.

© 2024 The Authors. Angewandte Chemie International Edition published by Wiley-VCH GmbH

15213773, 2024, 27, Downloaded from https://onlinelibrary.wiley.com/doi/10.1002/anie.202404972 by Leiden University Libraries, Wiley Online Library on [29/07/2024]. See the Terms and Conditions (https://onlinelibrary.wiley.com/terms-and-conditions) on Wiley Online Library for rules of use; OA articles are governed by the applicable Creative Commons License

[61] Y. Li, J. N. Hoskins, S. G. Sreerama, S. M. Grayson, *Macromolecules* **2010**, *43*, 6225–6228.
[62] C. Enjalbal, P. Ribière, F. Lamaty, N. Yadav-Bhatnagar, J. Martinez, J. L. Aubagnac, *J. Am. Soc. Mass Spectrom.* **2005**, *16*, 670–678.
[63] M. Vergaelen, *Poly(2-Oxazoline)s as Matrix Excipient for Solid Dispersions as New Drug Formulation Platform*, Ghent University, **2018**.
[64] J. Michalak, H. Bin Zhai, M. S. Platz, *J. Phys. Chem.* **1996**, *100*, 14028–14036.
[65] J. Dommerholt, F. P. J. T. Rutjes, F. L. Van Delft, *Top. Curr. Chem.* **2016**, *374*, 1–20.
[66] E. Leyva, S. Leyva, E. Moctezuma, R. M. González-Balderas, D. De Loera, *J. Fluorine Chem.* **2013**, *156*, 164–169.
[67] E. Leyva, M. S. Platz, S. E. Loredo-Carrillo, J. Aguilar, *Curr. Org. Chem.* **2020**, *24*, 1161–1180.
[68] B. Komarova, S. Maryasina, Y. Tsvetkov, N. Nifantiev, *Synthesis* **2013**, *45*, 471–478.
[69] J. V. Staros, H. Bayley, D. N. Standring, J. R. Knowles, *Biochem. Biophys. Res. Commun.* **1978**, *80*, 568–572.
[70] C. Gao, Z. B. Fisher, K. J. Edgar, *Cellulose* **2019**, *26*, 445–462.
[71] A. Dirisala, S. Uchida, J. Li, J. F. R. Van Guyse, K. Hayashi, S. V. C. Vummaleti, S. Kaur, Y. Mochida, S. Fukushima, K. Kataoka, *Macromol. Rapid Commun.* **2022**, 2100754.
[72] P. Mi, K. Miyata, K. Kataoka, H. Cabral, *Adv. Ther.* **2021**, *4*, 1–29.
[73] P. Wen, W. Ke, A. Dirisala, K. Toh, M. Tanaka, J. Li, *Adv. Drug Delivery Rev.* **2023**, *198*, 114895.
[74] S. Zalipsky, C. B. Hansen, J. M. Oaks, T. M. Allen, *J. Pharm. Sci.* **1996**, *85*, 133–137.
[75] B. Mui, Y. Tam, M. Jayaraman, S. Ansell, X. Du, Y. Tam, P. Lin, S. Chen, J. Narayanannair, K. Rajeev, M. Manoharan, A. Akinc, M. Maier, P. Cullis, T. Madden, M. Hope, *Mol. Ther. Nucleic Acids* **2013**, *2*, e139.
[76] S. A. Dilliard, Q. Cheng, D. J. Siegwart, *Proc. Natl. Acad. Sci. USA* **2021**, *118*, DOI 10.1073/pnas.2109256118.
[77] D. M. Strelkova Petersen, N. Chaudhary, M. L. Arral, R. M. Weiss, K. A. Whitehead, *Eur. J. Pharm. Biopharm.* **2023**, *192*, 126–135.
[78] R. Luxenhofer, R. Jordan, *Macromolecules* **2006**, *39*, 3509–3516.
[79] A. Gress, A. Völkel, H. Schlaad, *Macromolecules* **2007**, *40*, 7928–7933.
[80] T.-X. X. Lav, P. Lemechko, E. Renard, C. Amiel, V. Langlois, G. Volet, *React. Funct. Polym.* **2013**, *73*, 1001–1008.
[81] K. Suzuki, Y. Miura, Y. Mochida, T. Miyazaki, K. Toh, Y. Anraku, V. Melo, X. Liu, T. Ishii, O. Nagano, H. Saya, H. Cabral, K. Kataoka, *J. Controlled Release* **2019**, *301*, 28–41.
[82] M. C. Woodle, C. M. Engbers, S. Zalipsky, *Bioconjugate Chem.* **1994**, *5*, 493–496.
[83] P. J. M. Bouten, D. Hertsen, M. Vergaelen, B. D. Monnery, M. A. Boerman, H. Goossens, S. Catak, J. C. M. Van Hest, V. Van Speybroeck, R. Hoogenboom, *Polym. Chem.* **2015**, *6*, 514–518.
[84] C. Alexis, C. Charnay, V. Lapinte, J. J. Robin, *Prog. Org. Coat.* **2013**, *76*, 519–524.
[85] D. R. Burfield, K. H. Lee, R. H. Smithers, *J. Org. Chem.* **1977**, *42*, 3060–3065.
[86] S. Abbasi, K. Kajimoto, H. Harashima, *Int. J. Pharm.* **2018**, *553*, 398–407.
[87] S. Watanabe, K. Hayashi, K. Toh, H. J. Kim, X. Liu, H. Chaya, S. Fukushima, K. Katsushima, Y. Kondo, S. Uchida, S. Ogura, T. Nomoto, H. Takemoto, H. Cabral, H. Kinoh, H. Y. Tanaka, M. R. Kano, Y. Matsumoto, H. Fukuhara, S. Uchida, M. Nangaku, K. Osada, N. Nishiyama, K. Miyata, K. Kataoka, *Nat. Commun.* **2019**, *10*, 1894.
[88] S. Hiki, K. Kataoka, *Bioconjugate Chem.* **2007**, *18*, 2191–2196.
[89] M. Glassner, D. R. D'Hooge, J. Young Park, P. H. M. Van Steenberge, B. D. Monnery, M. F. Reyniers, R. Hoogenboom, *Eur. Polym. J.* **2015**, *65*, 298–304.
[90] M. W. M. Fijten, R. Hoogenboom, U. S. Schubert, *J. Polym. Sci. Part A* **2008**, *46*, 4804–4816.
[91] F. Wiesbrock, R. Hoogenboom, M. A. M. Leenen, M. A. R. Meier, U. S. Schubert, *Macromolecules* **2005**, *38*, 5025–5034.
[92] O. Nuyken, G. Maier, A. Groß, H. Fischer, *Macromol. Chem. Phys.* **1996**, *197*, 83–95.
[93] O. Sedlacek, B. D. Monnery, R. Hoogenboom, *Polym. Chem.* **2019**, *10*, 1286–1290.
[94] V. Kováčik, Š. Bauer, J. Rosík, P. Kováč, *Carbohydr. Res.* **1968**, *8*, 282–290.
[95] P. Wolkoff, S. Hammerum, *Org. Mass Spectrom.* **1976**, *11*, 375–382.

Manuscript received: March 13, 2024
Accepted manuscript online: April 23, 2024
Version of record online: June 3, 2024

© 2024 The Authors. Angewandte Chemie International Edition published by Wiley-VCH GmbH

15213773, 2024, 27, Downloaded from https://onlinelibrary.wiley.com/doi/10.1002/anie.202404972 by Leiden University Libraries, Wiley Online Library on [29/07/2024]. See the Terms and Conditions (https://onlinelibrary.wiley.com/terms-and-conditions) on Wiley Online Library for rules of use; OA articles are governed by the applicable Creative Commons License